Acta Crystallographica Section D
**Biological Crystallography**
ISSN 0907-4449

# Crystallization and preliminary X-ray study of OXA-1, a class D $\beta$-lactamase

**Tao Sun, Michiyoshi Nukaga, Kayoko Mayama, Gregg V. Crichlow, Alexandre P. Kuzin† and James R. Knox***

Department of Molecular and Cell Biology, The University of Connecticut, Storrs, Connecticut 06269-3125, USA

† Current address: Southern Research Institute, Birmingham, AL 35255, USA.

Correspondence e-mail: knox@uconnvm.uconn.edu

Received 27 July 2001
Accepted 2 October 2001

The *Escherichia coli* OXA-1 oxacillinase, a $\beta$-lactamase which provides resistance to $\beta$-lactam antibiotics (penicillins and cephalosporins), has been crystallized. A member of the class D family of serine $\beta$-lactamases, OXA-1 is especially active against the penicillins oxacillin and cloxacillin and is now found in 10% of *E. coli* clinical isolates. Crystals grown from PEG 8000 at pH 7.5 diffract to 1.5 Å resolution at 100 K and have space group $P1$ ($Z = 2$), with unit-cell parameters $a = 36.0$, $b = 51.6$, $c = 72.9$ Å, $\alpha = 70.2$, $\beta = 84.1$, $\gamma = 81.5^\circ$.

## 1. Introduction

$\beta$-Lactam antibiotics block bacterial cell-wall synthesis by inhibiting a D-Ala-D-Ala-carboxypeptidase/transpeptidase which cross-links neighboring peptidoglycan strands (Massova & Mobashery, 1998). The effectiveness of a $\beta$-lactam depends on its susceptibility to hydrolysis by bacterial $\beta$-lactamases, commonly called penicillinases or cephalosporinases, depending on specificity. Structural differences between the two types of $\beta$-lactamases have been described (Lobkovsky *et al.*, 1993), as well as their evolution from the cell-wall cross-linking enzymes (Knox *et al.*, 1996). $\beta$-Lactamases are grouped into four classes (A, B, C and D) based primarily on sequence (Bush & Mobashery, 1998). The serine-reactive $\beta$-lactamases (A, C and D) rapidly hydrolyze the $\beta$-lactam bond *via* an acyl intermediate to give an inactive acid. The class D $\beta$-lactamases are called oxacillinases because of their high-level activity against oxacillin and cloxacillin.

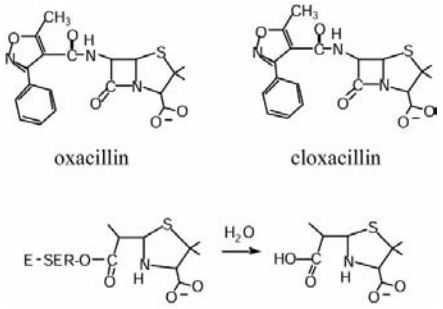


Approximately 24 class D enzymes are known and are designated OXA-1, OXA-2 *etc*. They have up to only 16% amino-acid identity with the more numerous enzymes of classes A and C (Naas & Nordmann, 1999). OXA-1 is the most common form and is found primarily in *Pseudomonas aeruginosa* and in enterobacteriaceae (Naas & Nordmann, 1999; Zhou *et al.*, 1994). This class D $\beta$-lactamase is poorly inhibited by clinically used suicide inhibitors such as clavulanic acid, sulbactam and tazobactam (Page, 2000; Payne *et al.*, 1994), but is readily inhibited by NaCl. Natural OXA variants (*e.g.* OXA-15, OXA-18 and OXA-19) have arisen with an expanded substrate spectrum which includes aztreonam and third-generation cephalosporins such as cefotaxime and ceftriaxone. This selection of variants, resistance to inhibitors and gene transfer *via* plasmids and integrons mean that oxacillinases are likely to become more widely dispersed among Gram-negative pathogens (Naas & Nordmann, 1999).

## 2. Experimental

### 2.1. Plasmid construction and protein purification

The OXA-1 gene was cloned from the RGN238 plasmid into pET12a-KM, which is a pET12a derivative with the original ampicillin-resistance marker replaced by one for kanamycin (pETKMOXA-1). All the signal sequence was removed and the $\beta$-lactamase was expressed to the cytoplasm of *E. coli* BL21 cells grown in M9CA broth containing kanamycin (50 $\mu$g ml$^{-1}$) at 303 K. Crude enzyme was purified using CM-Sephadex C-50, PBE94 and Sephadex G-75. Purity was estimated from SDS–PAGE gels to be more than 95%.

### 2.2. Crystallization

Crystals having prism morphology were grown at room temperature by the sitting-drop vapor-diffusion method. A 10 $\mu$l drop (2.5–3 mg ml$^{-1}$ protein, 10% PEG 8000, 0.05 *M* HEPES buffer pH 7.5) was placed over

0.75 ml reservoir solution containing 20% PEG, 0.1 *M* HEPES buffer pH 7.5. The 0.1–0.3 mm needle crystals appeared in one week. After streak and macro seeding, the crystals grew to 0.5 × 0.1 × 0.05 mm (Fig. 1). Twinning was common and data crystals had to be carefully selected under polarized light.

### 2.3. Collection of native X-ray data

Data to 1.5 Å resolution were collected at 100 K at CHESS station A1 at Cornell University. Two crystals were used to collect high- and low-resolution data sets. Reduction and merging of the two data sets with the *HKL* programs (Otwinowski & Minor, 1997) showed a data redundancy of 2.6 for this triclinic cell (Table 1). $R_{\rm merge}(I)$ for all data is 4.9%.

### 2.4. Collection of data from a uranyl derivative

Data from an OXA-1 crystal soaked in 1 m*M* $K_3UO_2F_5$ for 6 h were collected at 100 K with a HISTAR multiwire detector on an RU-200 rotating-anode generator. Data to 2.7 Å resolution were reduced and scaled by *XGEN* (Molecular Simulations Inc.) to an $R_{\rm merge}$ of 5.4%. Three-wavelength MAD data from the uranyl derivative were collected near the $L_{\rm III}$ edge to 2.3 Å resolution at NSLS station X4A at Brookhaven National Laboratory.

## 3. Results

### 3.1. Unit cell

The crystals have space group *P*1, with unit-cell parameters $a$ = 36.0, $b$ = 51.6, $c$ = 72.9 Å, $\alpha$ = 70.2, $\beta$ = 84.1, $\gamma$ = 81.5°. Diffraction to $d_{\rm min}$ = 1.5 Å is seen in synchrotron data. With an MW of 28.2 kDa and two molecules in the triclinic cell, the $V_{\rm M}$ and solvent content are found to be 2.24 Å$^3$ Da$^{-1}$ and 44%, respectively. The crystals can be cryoprotected with a 2–10 min immersion in buffered PEG containing 25% 2-methyl 2,4-pentanediol.

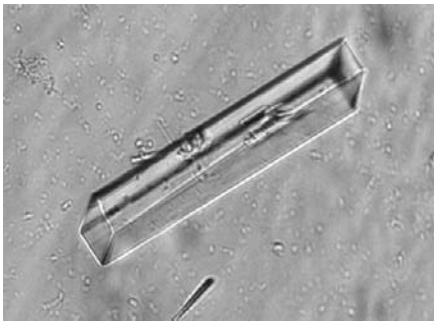

**Figure 1**
Crystal of OXA-1 oxacillinase grown by vapor diffusion from 10% PEG 8000 in 0.05 *M* HEPES buffer pH 7.5. The longest crystal dimension is 0.25 mm.

**Table 1**
X-ray data summary for OXA-1.

| | Native† | Uranium | MAD uranium | | |
|---|---|---|---|---|---|
| Wavelength (Å) | 0.935 | 1.542 | 0.7222 (inflection) | 0.7220 (peak) | 0.7171 (remote) |
| Resolution (Å) | 1.5 | 2.7 | — | 2.3 | — |
| Observations | 183270 (4561) | 30700 | 80145 | 63357 | 78416 |
| Reflections | 69838 (2979) | 11461 | 21328 | 21121 | 21331 |
| Compleness (%) | 86.5 (36.9) | 80.0 | 99.0 | 98.2 | 99.0 |
| $I/\sigma(I)$ | 20.8 (5.9) | 33.5 | 12.5 | 13.7 | 10.6 |
| $R_{\rm merge}$ (%) | 4.9 (12.3) | 5.4 | 8.7 | 6.2 | 9.9 |

† Data for 1.55–1.50 Å shell is in parentheses.

### 3.2. Self-rotation search

Analysis of the native data using *AMoRe* (Navaza, 1994) indicated that the two molecules in the triclinic cell are related by a 180° rotation about an axis approximately perpendicular to *a* and along the short *bc* diagonal.

### 3.3. Molecular-replacement search

Two recent crystal structures of OXA-10 (PDB codes 1fof and 1e4d) were used as search models for OXA-1. Six residues from the N- and C-termini were omitted from the model, as were about 40 residues in presumably flexible segments between secondary structure. The search using *EPMR* (Kissinger, 1999) used 4–15 Å data and confirmed the dyad axis found by the self-rotation function and showed a large 36 Å translation of the second molecule parallel to the dyad axis. For this initial solution, the correlation coefficient and crystallographic *R* factor were 0.22 and 0.59, respectively. Manual fitting and refinement by simulated annealing (Brunger *et al.*, 1998) were unsuccessful in reducing *R* and $R_{\rm free}$ to below 0.42 and 0.46, respectively, at 3.0 Å resolution. This difficulty may reflect the fact that significant differences exist between the monomeric OXA-1 and dimeric OXA-10 molecules. Amino-acid identity between the two is only 24% and there are four insertions totaling 14 residues in OXA-1 relative to OXA-10.

### 3.4. Patterson analysis of uranium data

Patterson maps using the single-wavelength data and $|F_{\rm uranyl} - F_{\rm native}|^2$ or $|\Delta F_{\rm uranyl\ \ anom}|^2$ as coefficients showed a strong U—U vector at $u$, $v$, $w$ = 0.14, 0.16, 0.38 which was 0.22 and 0.15 of the origin peak, respectively.

### 3.5. Phasing by MAD with uranium data

From the three-wavelength MAD data, the program *SOLVE* (Terwillinger & Berendzen, 1999) found the same two uranium sites. This two-site solution had a *Z* score of 37 and a figure of merit of 0.59. Phases to 2.7 Å resolution were calculated. The electron density of the Fourier map had poor correlation of neighboring density. Solvent flattening improved the map somewhat, but not enough to produce a refinable structure.

## 4. Discussion

To improve the map of the OXA-1 structure, we will make the selenomethionine-substituted protein for MAD data collection. It is expected that the covalency and high occupancy of Se atoms (six per 28.2 kDa) will provide better MAD data than were obtained from the uranium derivative.

Once the native structure is refined, we plan to study the unusual inactivation of the enzyme by chloride (Dale, 1971) by examining a series of crystal structures as a function of salt concentration. Understanding the role of chloride, whether in protein conformation or in substrate binding, may provide clues for inhibitor design.

Two published OXA-10 structures differ somewhat: in one, a divalent transition metal is seen bridging the dimer interface (Paetzel *et al.*, 2000; Danel *et al.*, 2001), but in the other structure the metal site is not seen (Maveyraud *et al.*, 2000). More importantly, one structure shows that a critical active-site lysine side chain is carbamylated (Maveyraud *et al.*, 2000), but carbamylation is not confirmed in the second structure. It is interesting that a catalytic role for carbamylation has been linked to the salt-induced inhibition discussed above, in that chloride binding in the active site is proposed to promote decarbamylation of the lysine and thus leads to inhibition (Maveyraud *et al.*, 2000). Resolution of these questions is

clearly needed for any discussion of the catalytic mechanism for the class D $\beta$-lactamases.

We thank Drs Paul Moews and Michael McDonough for assistance. Native data were collected with the assistance of Marian Szebenyi at station A1 at the Cornell High Energy Synchrotron Source (CHESS), which is supported by the NSF under award DMR-97-13424, using the Macromolecular Diffraction facility (MacCHESS), which is supported by award RR-01646 from the NIH. MAD data were collected with the help of Craig Ogata at station X4A at NSLS at Brookhaven National Laboratory, which is supported by the US Department of Energy, Division of Materials Sciences and the Division of Chemical Sciences.

## References

Brunger, A. T., Adams, P. D., Clore, G. M., Delano, W. L., Gros, P., Grosse-Kunstleve, R. W., Jiang, J.-S., Kuszewski, J., Nilges, M., Pannu, N. S., Read, R. J., Rice, L. M., Simonson, T. & Warren, G. L. (1998). *Acta Cryst.* D**54**, 905–921.

Bush, K. & Mobashery, S. (1998). *Resolving the Antibiotic Paradox*, edited by B. Rosen & S. Mobashery, pp. 71–98. New York: Kluwer Academic/Plenum.

Dale, J. W. (1971). *Biochem. J.* **123**, 501–505.

Danel, F., Paetzel, M., Strynadka, N. C. J. & Page, M. G. P. (2001). *Biochemistry*, **40**, 9412–9420.

Kissinger, C. R. (1999). *Acta Cryst.* D**55**, 484–491.

Knox, J. R., Moews, P. C. & Frere, J.-M. (1996). *Chem. Biol.* **3**, 937–947.

Lobkovsky, E., Moews, P. C., Liu, H., Zhao, H., Frere, J.-M. & Knox, J. R. (1993). *Proc. Natl. Acad. Sci. USA*, **90**, 11257–11261.

Massova, I. & Mobashery, S. (1998). *Antimicrob. Agents Chemother.* **42**, 1–17.

Maveyraud, L., Golemi, D., Kotra, L. P., Tranier, S., Vakulenko, S., Mobashery, S. & Samama, J.-P. (2000). *Structure*, **8**, 1289–1298.

Naas, T. & Nordmann, P. (1999). *Curr. Pharmacol. Des.* **5**, 865–879.

Navaza, J. (1994). *Acta Cryst.* A**50**, 157–163.

Otwinowski, Z. & Minor, W. (1997). *Methods Enzymol.* **276**, 307–326.

Paetzel, M., Danel, F., Castro, L., Mosimann, S. C., Page, M. G. P. & Strynadka, N. C. J. (2000). *Nature Struct. Biol.* **7**, 918–925.

Page, M. G. P. (2000). *Drug Resist. Updat.* **3**, 109–125.

Payne, D. J., Cramp, R., Winstanley, D. J. & Knowles, D. J. C. (1994). *Antimicrob. Agents Chemother.* **38**, 767–772.

Terwilliger, T. C. & Berendzen, J. (1999). *Acta Cryst.* D**55**, 849–861.

Zhou, X. Y., Bordon, F., Sirot, D. & Kitz, C. R. (1994). *Antimicrob. Agents Chemother.* **38**, 1085–1089.